Impact of the external window crack structure on indoor $PM_{2.5}$ mass concentration

Ziguang Chen[a], Chao Chen[a,*], Shen Wei[b], Yuqin Wu[a], Yafeng Wang[a], Yali Wan[a]

[a] *College of Architecture and Civil Engineering, Beijing University of Technology, Beijing, P R China, 100024*

[b] *Department of Mechanical and Construction Engineering, Northumbria University, Newcastle-upon-Tyne, UK, NE1 8ST*

[*]*Corresponding author: Chao Chen, Tel: +86 10 67391608-201; Fax: +86 10 67391608-201.*

E-mail address: chenchao@bjut.edu.cn

Abstract:

The fine particulate matter, generally known as $PM_{2.5}$, has great impact on the air quality and human health. Although closing external windows can help prevent outdoor $PM_{2.5}$ going into indoors, many studies have shown that a significant number of particles can still pass the building façade through the cracks around the window. In order to quantify the influence of the external window crack structure and some relevant parameters, such as room dimension, on the indoor $PM_{2.5}$ mass concentration, this paper introduces an updated model from a previously published paper by the authors (Zhao et al., 2015). The model was developed based on two-month field measured data from five unoccupied offices located in the central area of Beijing (capital city located in northern China), and then was validated against a new dataset measured in Guangzhou (a major city located in

southern China). The model can be used to quantify the indoor $PM_{2.5}$ mass concentration based on the instant outdoor $PM_{2.5}$ level, considering influences from external window crack structure, room dimension and outdoor meteorological conditions, i.e. outdoor wind speed and relative humidity.

Key words:

Air pollution; $PM_{2.5}$; Window crack structure; Infiltration; $PM_{2.5}$ modeling

1. Introduction

In the past few decades China has experienced a rapid development in both urbanization and industrialization, especially in the Beijing-Tianjin-Hebei (BTH) region. This fast growth of economy has brought many development opportunities but meanwhile has also led to serious air pollution issues. The fine particulate matter ($PM_{2.5}$) is currently of greatest concern in China in terms of both atmospheric air quality and human health [1]. According to the China Environmental Status Bulletin published in 2015 [2], $PM_{2.5}$ is the primary pollutant in the BTH region recently, which is the most polluted area in China. In Beijing, the central area of the BTH region, the annual mean value of atmospheric $PM_{2.5}$ mass concentration was 80.6μg/m³, over two times of the annual allowance recommended by the WHO (35μg/m³) [3]. Epidemiologic evidence has revealed the significant impact of the exposure time under $PM_{2.5}$ pollution on human's heath, as it may lead to serious health problems, such as asthma, chronic obstructive pulmonary disease and lung cancer [4]. In current society, most people are spending over 90% time inside

buildings. Therefore, providing an indoor environment with acceptable $PM_{2.5}$ mass concentration is essential for a good built environment.

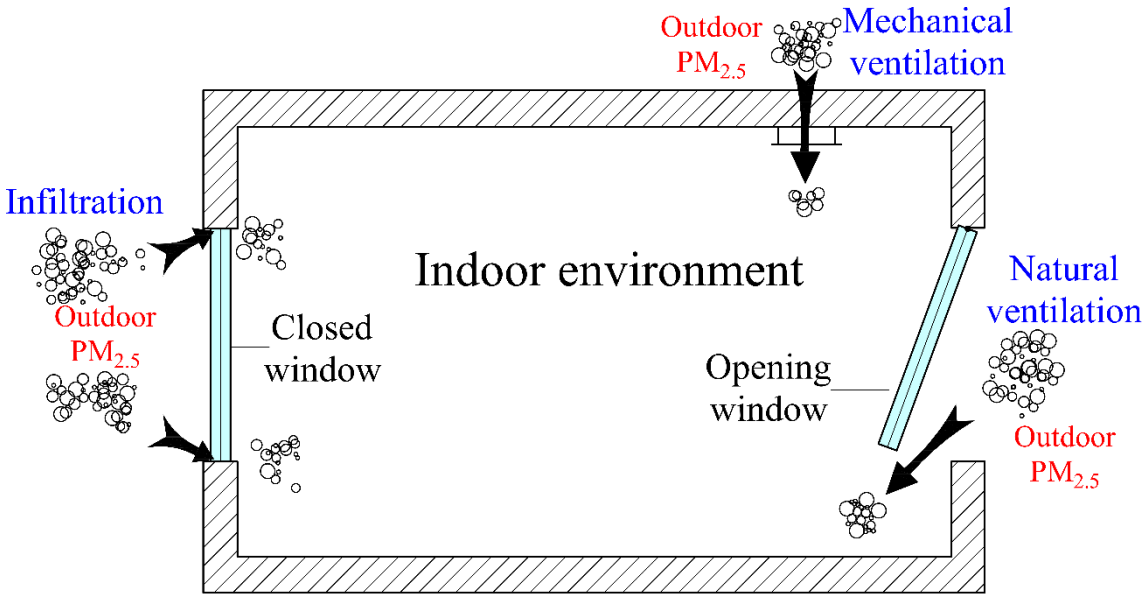

Figure 1: Main routes for outdoor $PM_{2.5}$ going into the indoor environment

Existing studies have suggested three principal routes of outdoor $PM_{2.5}$ going indoors [5]. These include mechanical ventilation, natural ventilation and infiltration, as shown in Figure 1. Mechanical ventilation is usually driven by fans to achieve the exchange of air between indoors and outdoors. During this process many particles can still go into the indoor environment through the system although filters are popularly used in real applications, aiming to stop the pass of pollutants. Natural ventilation can be driven by both wind pressure and temperature difference and generally there is no filters installed to prevent the pass of pollutants. Under this system, the most popular way of preventing $PM_{2.5}$ going into indoors is closing all external windows to reduce the air exchange between indoors and outdoors [6]. Infiltration refers to those air exchanges through the cracks and small holes inside the building fabric. Although this part of air exchange is

small, the amount of particles imported through infiltration is also sufficient to cause indoor air pollution [7]. $PM_{2.5}$ penetration through this part, however, is almost not controllable by people's interaction with the building systems.

Most existing studies on the barrier property of buildings' fabric against $PM_{2.5}$ pollution were based on field measured data from real buildings. These studies have been carried out in various buildings, such as education buildings [8-15], office buildings [16-21] and residential buildings [22-25]. These studies mainly focused on evaluating the correlation between indoor and outdoor $PM_{2.5}$ mass concentrations, under various physical conditions. Although many useful results have been gained from these studies, their application is much dependent on the experimental conditions when and where the data were collected so cannot be used in a more general situation.

In order to cover the above issue, some studies have tried to develop models that can link indoor and outdoor pollution levels based on important influential factors [26-36]. These factors include outdoor meteorological conditions [26-30], building façade properties [31-35] and occupant behavior [35, 36]. In order to evaluate the barrier property of important building façade components against outdoor pollutants, such as for the external window crack structure, Liu et al. [32] have proposed a theoretical model for calculating the penetration factor (P) of building fabric crack under various particle sizes. Following this model, Tian et al. [33] proposed a correction method for the crack roughness used in the model, based on the boundary layer thickness. Then Chen et al. [34] carried out a

further development on this method, enabling the calculation of the particle penetration factor under various particle sizes for actual engineering applications. These models, however, are all dependent on the particle sizes and cannot be used to calculate a mean penetration factor for all particles less than 2.5μm, which are those considered as $PM_{2.5}$. This limits their applicability of estimating the barrier property of an actual building façade against outdoor $PM_{2.5}$. Additionally, due to the significant impact of external window air-tightness level on the correlation between indoor and outdoor $PM_{2.5}$ mass concentrations [18, 37], penetration factors (*P*) calculated under various particle sizes cannot quantify the individual influence of external window air-tightness level, external window crack structure and other relevant parameters, such as room dimension, on the indoor $PM_{2.5}$ mass concentration. Therefore, a suitable evaluation method that can handle the above issues are highly required to be developed.

According to the research issues mentioned above, the research team of this paper has already carried out a study in one office building in Beijing, China, and developed a predictive model considering the combinational influence of external window crack structure, room dimension and outdoor meteorological conditions [18]. In that model, a comprehensive structure characteristic coefficient, *A*, has been adopted to reflect the influence of two important parameters, i.e. external window crack structure and room dimension, on the indoor $PM_{2.5}$ mass concentration (details can be found in Section 2.1). However, the coefficient *A* in that model is a value combining the influence of both external window crack structure and room dimension and developed by statistical

analysis method. Therefore, when one parameter is changed new field data have to be collected for developing another *A* for the new application, which limits the flexibility of the method. Additionally, as the coefficient *A* combines the impact of two influential parameters, i.e. external window crack structure and room dimension, on the indoor $PM_{2.5}$ mass concentration, the individual contribution of each parameter cannot be separately reflected by the model. Under this condition, a more general method to link *A* with some easy-to-obtain parameters, such as building properties (e.g. window crack structure and room dimension), is highly required.

In order to make the existing method more flexible by considering the individual influence from external window crack structure and room dimension, this study adopted a method that can be used to calculate the value of *A* based on the building's external window crack structure and room dimension, which is easier to be obtained. The method was developed using field measured data from six different buildings (five buildings were used to provide data for the model development, while one building was used for model validation), monitored continuously in a two-month period. With this method, the updated model can then be used to analyze the indoor $PM_{2.5}$ mass concentration under various external window crack structures and room dimensions.

2. Methodology

2.1 Existing model description

A detailed introduction of the existing model has been published recently [18], and the

model can be expressed as Equation 1,

$$\frac{I_i}{O_i} = A \cdot \left(\frac{U_i}{\exp \overline{\ln(U_i)}} \right)^B \cdot \left(\frac{RH_i}{\exp \overline{\ln(RH_i)}} \right)^C \quad (1)$$

where I_i/O_i is the mean Indoor/Outdoor ratio; U_i is the outdoor wind speed around the sampling site (in m/s) and RH_i is the outdoor relative humidity around the sampling site (in %). *A* is the coefficient mentioned above, considering the combinational influence of the external window crack structure and room dimension. *B*, *C* are two correction factors for outdoor wind speed and relative humidity, respectively. In the published paper, the reliability of using this method to predict the I/O ratio of $PM_{2.5}$ mass concentration has been demonstrated.

2.2 Further development of coefficient A

In order to solve the two issues described in the introduction section, the coefficient *A* in Equation 1 was further developed in this study, linking it with the two important parameters, i.e. external window crack structure and room dimension.

2.2.1 Linking coefficient A with the two parameters

Studies have justified that the amount of pollutants entering indoors is dependent on three main factors [38], namely, air infiltration rate (*a*), penetration factor (*P*) and deposition rate (*k*). During the infiltration process, the indoor $PM_{2.5}$ mass concentration follows the mass balance principle defined by Equation 2, ignoring any coagulation and phase change

process and indoor pollutant source,

$$\frac{\mathrm{d}C_{in}}{\mathrm{d}t} = aPC_o - kC_{in} - aC_{in} \quad (2)$$

where C_{in}, C_o are indoor and outdoor $PM_{2.5}$ mass concentrations, respectively (in μg/m³); a is the air infiltration rate (in ACH); P is the particles' penetration factor (dimensionless); k is the particles' deposition factor (in h^{-1}).

Under steady-state conditions, it is acceptable that Equation 2 equals to 0 [39], so

$$aPC_o - kC_{in} - aC_{in} = 0 \quad (3)$$

Rearranging Equation 3 can get Equation 4, which links I/O ratio with a, P and k,

$$\frac{I}{O} = \frac{C_{in}}{C_o} = \frac{aP}{a+k} \quad (4)$$

Substituting Equation 4 into Equation 1 can obtain the relationship defined by Equation 5,

$$\frac{aP}{a+k} = A \cdot \left(\frac{U_i}{\exp\overline{\ln(U_i)}} \right)^B \cdot \left(\frac{RH_i}{\exp\overline{\ln(RH_i)}} \right)^C \quad (5)$$

For a given building, air infiltration rate (a) reflects the amount of air exchanged between indoors and outdoors through infiltration, so it also determines the amount of outdoor particles getting through the cracks around external windows. According to the basic ventilation theory [40], under infiltration condition, the air exchanging rate (a) is mainly dependent on the pressure difference between the two sides of an external window, caused by wind force and buoyancy force. Therefore, it is mainly influenced by outdoor meteorological parameters [41-44]. Penetration factor (P) is defined as the fraction of particles in the infiltration air passing through the window crack, and it is directly linked with the external window crack structure [32, 45-47]. The deposition rate (k) reflects the indoor suspended particles concentration decay rate since natural sedimentation, and it is mainly affected by the zonal dimension and structure under stable conditions (no ventilation and air disturbance) [48-50]. According to these, it can be generally considered that in Equation 5, the infiltration rate (a) is mainly dependent on the terms related to outdoor weather conditions, i.e. $a=f(U, RH)$; the coefficient A is mainly dependent on the P and k, i.e. $A=f(P, k)$, so $A=f$(external window crack structure, room dimension).

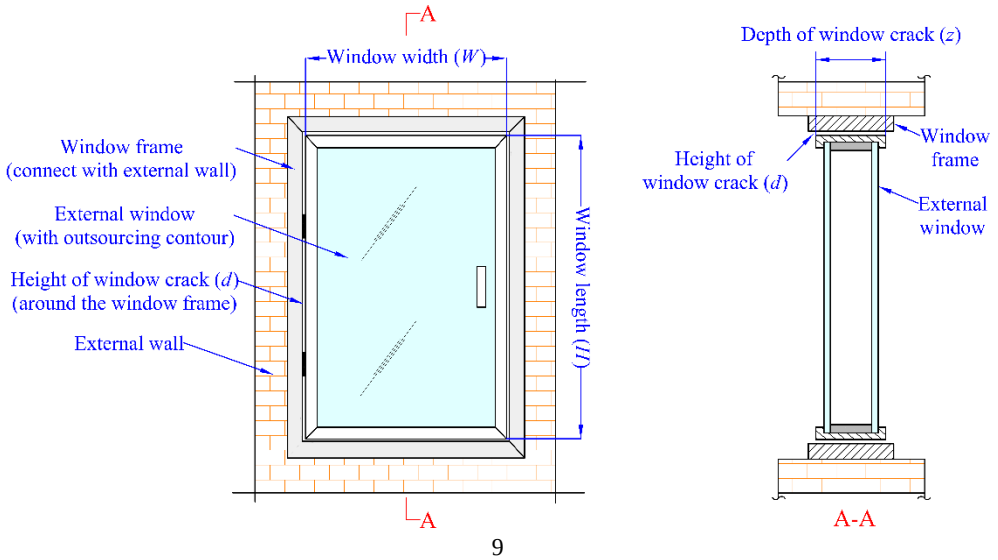

Figure 2: Schematic diagram of an example external window

2.2.2 Correlating A with external window crack structure

Figure 2 above depicts a schematic drawing of a typical external window, in order to show important parameters that will be used in the following analysis. As described already, linking *A* with external window crack structure was mainly achieved through the penetration factor (*P*). Generally, there are three kinds of resistance when particles penetrating through a window crack, and they are gravity sedimentation, brown diffusion and inertial impaction [32-34]. Existing studies have shown that the inertial impaction is not an important particle deposition mechanism for airflow through building cracks and so it was ignored in the study. The penetration factor, therefore, was calculated based on gravity sedimentation (P_g) and Brown diffusion (P_B), as shown in Equation 6,

$$P = P_g \cdot P_B \tag{6}$$

where P_g and P_B can be calculated by Equations 7 and 8 following [32-34],

$$P_g = 1 - \frac{z}{d} \cdot \frac{v_s}{u_m} \tag{7}$$

$$P_B = 0.915\exp\left(-1.885\varphi\right) + 0.0592\exp\left(-22.3\varphi\right) + 0.026\exp\left(-152\varphi\right) \tag{8}$$

where, z and d are the depth and height of the external window crack (in m). u_{m} and v_{s} are

the air flow speed and the gravitational sedimentation velocity in the crack (in m/s). φ is a dimensionless coefficient and $\varphi = \frac{4Dz}{d_p^2 u_m}$. D is the Brown diffusion coefficient (in m^2/s) and d_p is the particle diameter (in m).

It should be noted that relevant studies have demonstrated that the air flow alongside a slender crack can be considered as laminar flow, and under this condition u_m is mainly influenced by the crack structure (z and d) [32, 51]. Besides, although the v_s and φ are dependent on the particle diameter, Popescu et al. [52] and He et al. [53] have suggested that the particles diameter has little impact on both penetration factor and deposition rate when the diameter is within 0.1-2.5μm. Therefore, the influence caused by the particle diameter was also ignored in this study, as this is the range defining $PM_{2.5}$.

Based on this assumption and Equations 6 to 8, z and d can suitably reflect the structural characteristics of external window cracks and particle penetration performance. Therefore, in this study, a characteristic dimension of penetration factor, noting as A_p, was suggested. It was defined as the ratio of the window crack sectional area, denoted as F_P ($PM_{2.5}$ accessible area, in m^2) to the surface area alongside the depth of the window crack, denoted as F_z ($PM_{2.5}$ deposition area, in m^2), as expressed in Equation 9. This value will be used later to couple the influence of external window crack structure to the coefficient A:

$$A_P = \frac{F_P}{F_z} = \frac{dL_w}{zL_w} = \frac{d}{z} \quad (9)$$

2.2.3 Correlating A with room dimension

Figure 3 depicts a schematic drawing of a typical room, in order to show important parameters that will be used in the following analysis.

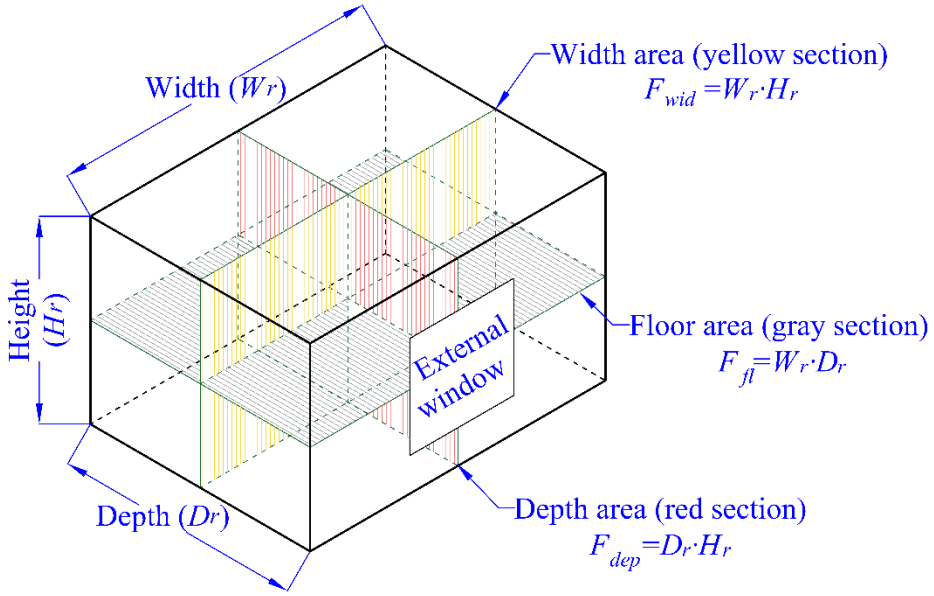

Figure 3: Schematic diagram of a typical room

As mentioned already, linking *A* with room dimension was mainly achieved through the deposition rate (*k*), because room dimension has a significant impact on the indoor particle deposition performance when there was no mechanical ventilation and internal disturbance (e.g. occupant behavior). According to a formula proposed by You et al. [54] for particle deposition velocity (Equation 10), a characteristic dimension of the deposition rate has been proposed in this study, noting as A_k. It was defined as the ratio of the room cross-sectional area in parallel to the external window, denoted as F_{wid} (in m^2), to the

deposition-weighted internal surface area, denoted as F_{wei} (in m^2). This definition was based on an assumption that particles pass through the external windows perpendicularly and then deposit onto each internal surface independently, as expressed in Equation 11.

$$v_d = \frac{\sum_{i=1}^{n} v_{di} F_i}{\sum F_i} \tag{10}$$

$$A_k = \frac{F_{wid}}{F_{wei}} = \frac{F_{wid}}{\sum F_i \cdot \varphi_i} = \frac{F_{wid}}{F_{fl}\left(\varphi_{ce} + \varphi_{fl}\right) + 2\left(F_{dep} + F_{wid}\right)\varphi_{ve}} \tag{11}$$

where φ_i is the deposition-weighted proportion factor (in %) as defined by Abadie et al. [55]; F_i is the surface area of each building internal surface (in m^2).

In the above equation, when defining the deposition-weighted internal surface area, F_{wei}, the particle deposition proportion to each surface was considered to be discrepant. Therefore, the deposition-weighted proportion factor, φ_i (in %), was brought into the equation, defined according to [55] for common wall components: most particles deposit onto the floor (φ_{fl}=60.6%±8.4%), followed by those onto the vertical walls (φ_{ve}=28.4%±3.0%), with those onto the ceiling to be least (φ_{ce}=11.0%±5.4%). $F_{wid}=H_r \cdot W_r$, denoted as the width area; $F_{dep}=H_r \cdot D_r$, denoted as the depth area; $F_{fl}=D_r \cdot W_r$, which is the floor area (see Figure 3).

2.3 Method development

In order to reflect the individual influence of P and k, shown in Equation 5, on the coefficient A, Equation 12 was developed,

$$A = \left(A_P\right)^{\gamma_1} \cdot \left(A_k\right)^{\gamma_2} \tag{12}$$

where γ_1, γ_2 are correction factors for A_P and A_k, respectively, which are dimensionless.

Then substituting Equation 9 and 11 into the above equation can obtain,

$$A = \left(\frac{d}{z}\right)^{\gamma_1} \cdot \left(\frac{F_{wid}}{F_{fl}\left(\varphi_{ce}+\varphi_{fl}\right)+2\left(F_{dep}+F_{wid}\right)\varphi_{ve}}\right)^{\gamma_2} \tag{13}$$

Apparently, A_p, A_k can be calculated using existing building parameters, such as external window crack structure and room dimension. As described by Zhao et al. [18], A can be derived from statistical analysis on field measurement data. However, γ_1, γ_2 are unknown variables in the equation. Thus, for n buildings, the following matrix can be established,

$$\begin{cases} A_1 = \left(A_{P_1}\right)^{\gamma_1} \cdot \left(A_{k_1}\right)^{\gamma_2} \\ A_2 = \left(A_{P_2}\right)^{\gamma_1} \cdot \left(A_{k_2}\right)^{\gamma_2} \\ \quad \mathrm{M} \\ A_i = \left(A_{P_i}\right)^{\gamma_1} \cdot \left(A_{k_i}\right)^{\gamma_2} \\ \quad \mathrm{M} \\ A_n = \left(A_{P_n}\right)^{\gamma_1} \cdot \left(A_{k_n}\right)^{\gamma_2} \end{cases} \tag{14}$$

Matrix 14 was rewritten as,

$$\begin{cases} \gamma_1 \cdot \ln\left(A_{P_1}\right) + \gamma_2 \cdot \ln\left(A_{k_1}\right) = \ln\left(A_1\right) \\ \gamma_1 \cdot \ln\left(A_{P_2}\right) + \gamma_2 \cdot \ln\left(A_{k_2}\right) = \ln\left(A_2\right) \\ \text{M} \\ \gamma_1 \cdot \ln\left(A_{P_i}\right) + \gamma_2 \cdot \ln\left(A_{k_i}\right) = \ln\left(A_i\right) \\ \text{M} \\ \gamma_1 \cdot \ln\left(A_{P_n}\right) + \gamma_2 \cdot \ln\left(A_{k_n}\right) = \ln\left(A_n\right) \end{cases} \tag{15}$$

Then the above matrix can be described as $\boldsymbol{A\gamma=b}$ (where, $\boldsymbol{A}$ is the Coefficient Matrix, $\boldsymbol{\gamma}$ is the matrix of unknown parameters and $\boldsymbol{b}$ is the Augmented Matrix). Since there are *n* equations and 2 unknowns only in the above matrix, according to the matrix theory, the Least Squares Method [56] can be used to solve the equations, given as $\boldsymbol{\gamma=(A^TA)^{-1}(A^Tb)}$. The model solution and validation are expressed in Section 3.2, using the data introduced in Section 3.1.

3. Case study

3.1 Data collection

In this study, data have been collected from six offices located in Beijing and GuangZhou, China. The data collected from Beijing offices were used to solve the above model while the one collected from GuangZhou was used for model validation. Details of the method can be found in the following sections.

3.1.1 Sampling sites

Figure 4a depicts the locations of the five sampling sites (five offices) of this study in Beijing, China, numbered from Sampling Site 1 (SP1) to Sampling Site 5 (SP5), and all the five sampling sites are located in the central area of Beijing. Figure 4b depicted the location of sampling site in Guangzhou, China, numbered as Sampling Site 6 (SP6). It is located in the central area of Guangzhou. In the study, all six offices have been monitored for about 2 months in winter with respect to both indoor and outdoor $PM_{2.5}$ mass concentrations. Throughout the monitoring period, all sampling sites were unoccupied, and had no air-conditioning and ventilation (with closed external windows and internal doors). Additionally, all walls of the six sampling sites were concrete construction, with insulation layer on the outer wall surface (the external walls of SP1-SP5 had 50mm insulation layer, and the external wall of SP6 had 30mm insulation layer). In addition, all walls had good compactness and there were no holes or cracks on the surfaces. According to these, it was considered in the study that the external window crack was the only route of air infiltration from outdoors to indoors. Meanwhile, in order to get rid of the air leakage from internal openings such as internal doors, all internal openings were closed during the measurement and all cracks around them were sealed using tapes.

Additionally, no electronic devices were running except the monitoring devices, in order to get rid of pollutants generated from those devices.

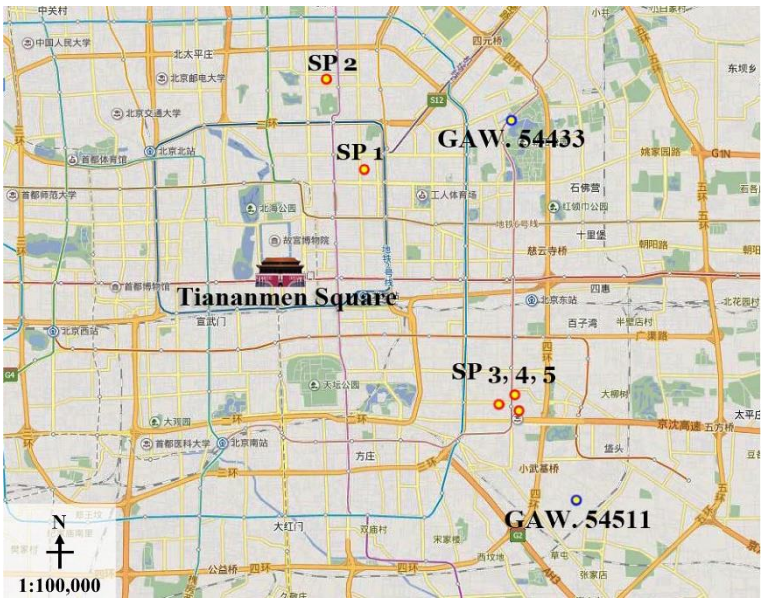

a) Locations of SP1-SP5 and the two GAW stations in Beijing

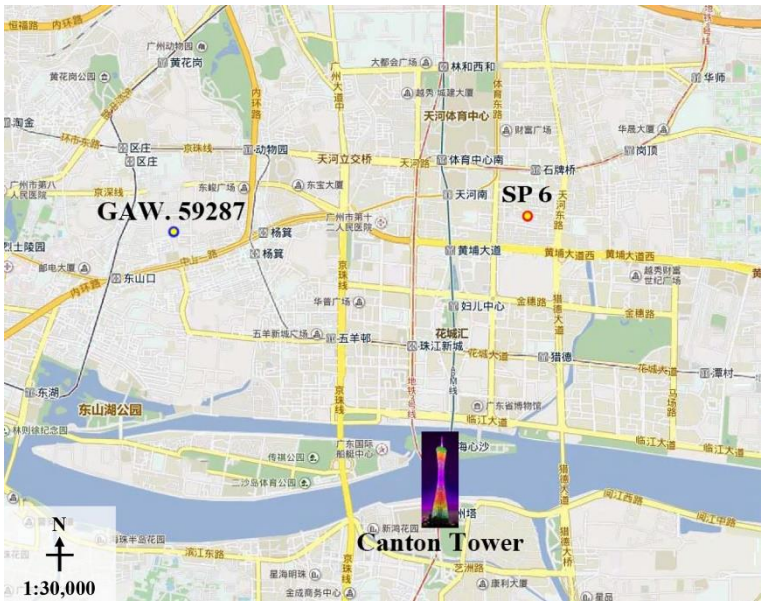

b) Location of SP6 and the GAW station in Guangzhou

Figure 4: Locations of the six sampling sites and the three GAW stations

Some detailed information about the external window crack structure and room dimension of the six sampling sites has been provided in Table 1. From Table 1, it can be found that the selected samples have various characteristics and locations, aiming to

justify the impact of various characteristics on the value of coefficient *A*, as well as the variation of γ_1 and γ_2 under different building conditions.

Table 1: The information about the six sampling sites in detail

Table 1

Sampling Site	Room dimension ($H_r \times W_r \times D_r$, mm)	Window types	Window air-tightness [a]	Window size ($H \times W$, mm) [b]	Crack depth z (mm)
1	2800×4500×4400	Casement	4	1150×700	50
2	3000×6000×4000	Casement	8	1200×900	70
3	3700×4400×5900	Sliding	3	1070×1160	62
4	2800×11800×8600	Casement	5	1800×1500	70
5	3300×6000×3000	Casement	6	1700×900	70
6	2800×4000×4000	Casement	4	1100×550	55

[a] The air-tightness of all external windows was evaluated by the China National Standard - GB/T 7106-2008, and more information can be found as follows.

[b] This size accounted the openable area of the window, while fixed windows were considered as a part of the external walls.

One of the biggest challenges of this study was to estimate the window crack height (*d*) for the windows in each sampling site, because this parameter is scarcely possible to measure using conventional measuring devices. To solve this issue, this study proposed a method based on the relationship between the window air-tightness level and the corresponding air infiltration rate on unit crack length (q_l, in $m^3/(m \cdot h)$), which has been defined in the China National Standard - *GB/T 7106-2008 Graduations and test methods*

of air permeability, watertightness, wind load resistance performance for building external windows and doors [57] (Table 2 has listed the mandatory indexsspecified in GB/T 7106-2008). Using the Table 2, the window crack height (d) was inversely calculated by subsituting the corresponding q_l to Equation 16, which is a common equation used by researchers when defining the relationship between the airflow rate and the crack structure [51]. Using this method, the calculated window crack heights for all six sampling sites were obtained and listed in Table 3.

It is worthy of noting that in order to get rid of the uncertainties caused by using theoretical values for real applications, all sampling sites were carefully chosen so their actual situation can strictly follow the Table 2 in the standard [57]. The considerations during the selection procedure included: 1) all windows' air-tightness were strictly determined by the standard when the buildings were designed and constructed; 2) all windows' air-tightness level has been inspected at the manufacturer to ensure strict compliance with the standard; 3) all buildings are newly-built so corrosions caused during the operation phase can be neglected.

$$\Delta p = \frac{12\mu z}{d^3} q_l + \frac{\rho(1.5+n)}{2d^2} q_l^2 \tag{16}$$

where, μ is the dynamic viscosity of air (in kPa·s); ρ is the air density (in kg/m³); n is the number of right-angle bends in the window crack; Δp is the pressure difference between the two window sides (in Pa).

Table 2: Air-tightness level of external window in GB/T 7106-2008

Table 2

Air-tightness level [a]	1	2	3	4	5	6	7	8
q_l [b]	3.5~4.0	3.0~3.5	2.5~3.0	2.0~2.5	1.5~2.0	1.0~1.5	0.5~1.0	≤0.5

[a] Air-tightness of external windows is defined as the property of infiltration air prevention when the external window is closed. The experimental condition used to develop the above table was under 10Pa pressure difference between the two sides of the window, at typical temperature (20℃) and pressure conditions (1atm).

[b] q_l represents the air infiltration rate on unit crack length, in $m^3/(m \cdot h)$. In this study, the mean value for each air-tightness level was adopted when estimating the window's crack height.

Table 3: Window crack heights for all six sampling sites

Table 3

Sampling Site	1	2	3	4	5	6
Window crack height (*d*) (mm)	0.912	0.599	0.910	0.819	1.054	0.939

3.1.2 Monitoring and data processing

In this study, both indoor and outdoor $PM_{2.5}$ mass concentrations were concurrently measured and recorded using LD-5C(R) line particle monitors, with a measurement range of 1 to $10^4 \mu g/m^3$ and sensitivity of $1 \mu g/m^3$. The sampling interval was 20 minutes, chosen based on a consideration of equipment maintenance. Although it is longer than that popularly adopted in previously studies, which is 5 minutes, a pilot study has demonstrated that there is no significant difference for data measured at 5 minutes interval and 20 minutes interval.

In the study, outdoor meteorological parameters, i.e. outdoor wind speed (U_i) and relative humidity (RH_i), were collected by regional Global Atmosphere Watch (GAW) stations at an hourly basis (http://data.cma.gov.cn/). In both Beijing and Guangzhou, there are a number of such stations distributed inside the city and the closest station for each sampling site was chosen as data provider. In order to handle the difference between local outdoor environment, especially for wind speed, and that at a nearby weather station, the ASHRAE method has been adopted to correct the wind speed values obtained from the station, as shown in Equation 17. This method has considered the impact of the height of the window, the local building terrain and the local wind boundary layer thickness of both the weather station and the sampling site, when correcting the data measured at a local weather station to be applicable for a local field application.

$$U_i = U_{\text{met}} \left(\frac{\delta_{\text{met}}}{h_{\text{met}}} \right)^{\alpha_{\text{met}}} \left(\frac{h_i}{\delta_i} \right)^{\alpha_i} \tag{17}$$

where, U_{met} is the wind speed measured at weather station, in m/s; δ_{met} and δ_i are the local wind boundary layer thickness of the weather station and the sampling site, respectively, in m, and the values have been determined according to [58]; h_{met} and h_i are the height of the weather station and the sampling site, respectively, in m; α_{met} and α_i are the exponent of the local building terrain of both weather station and the sampling site, which is dimensionless, and the values used in this study were also coming from [58]. Table 4 has listed all values chosen in this study for the calculation of Equation 17.

Table 4: Detail values in Equation 17 for the six samplings sites and the three GAW stations

Table 4

Location	h_{met} or h_i (m)	δ_{met} or δ_i (m)	α_{met} or α_i
GAW 54433	10	270	0.14
GAW 54511	15	210	0.1
GAW 59287	15	370	0.22
SP1	28	460	0.33
SP2	45	370	0.22
SP3	30	370	0.22
SP4	23	370	0.22
SP5	20	370	0.22
SP6	25	460	0.33

A number of existing studies have revealed a strong inverse relationship between wind speed and outdoor $PM_{2.5}$ mass concentration, that is to say a high outdoor wind speed leads to a low level of pollution [14, 15, 29]. Due to the target of this study, only high pollution circumstances have been used for the later analysis (concentration >115μg/m^3). Under this condition, the wind speed was low, which leads to an ignorance of the impact from wind direction, as suggested in [44].

Due to the different sampling intervals of $PM_{2.5}$ mass concentrations (both indoors and outdoors) and meteorological parameters, in the later data analysis, the measured $PM_{2.5}$ mass concentrations were averaged on the basis of every hour, in order to be consistent with the measured outdoor meteorological parameters.

3.1.3 *Measurement conditions*

This study focused on the winter time, as it has the most serious $PM_{2.5}$ pollution of the

year in both Beijing and Guangzhou [2]. The monitoring data of SP1 and SP2 were selected between 1st Nov to 30th Dec, 2015. Meanwhile the monitoring data of SP3-SP5 were selected between 1st Jan to 29th Feb, 2016. The monitoring data of SP6 were selected between 1st Dec, 2014 and 30th Jan, 2015. Beijing is located in northern China (39.8°N, 116.5°E), belonging to the zone of typical continental monsoon climate. During the monitoring period, the outdoor temperature was ranging between -16.8℃ and 16.0℃, with a mean value of -0.4℃. The relative humidity was ranging between 10% and 95%, with a mean value of 56%. The measured wind speed was mainly falling within 0 and 6.6m/s, with a mean value of 1.3m/s. Guangzhou, however, is located in the southern coastal area of China (23.1°N, 112.9°E), belonging to the zone of typical subtropical monsoon climate. This choice can reflect the applicability of the developed model in another location or climatic condition. During the monitoring period, the outdoor temperature was ranging between 1.3℃ and 24.2℃, with a mean value of 12.7℃. The relative humidity was ranging between 15% and 99%, with a mean value of 69%. The measured wind speed was mainly falling within 0 and 6.1m/s, with a mean value of 1.1m/s.

Figure 5a depicts the outdoor $PM_{2.5}$ mass concentration for the whole monitoring period in Beijing (Nov, 2015 to Feb, 2016). The highest $PM_{2.5}$ mass concentration reached 558μg/m³, and the mean $PM_{2.5}$ mass concentration was 103.7μg/m³. In Guangzhou, Figure 5b depicts the outdoor $PM_{2.5}$ mass concentration for the whole monitoring period between Dec, 2014 and Jan, 2015. The highest $PM_{2.5}$ mass concentration has reached 294μg/m³, and the mean $PM_{2.5}$ mass concentration was 91.3μg/m³. According to the

classification method proposed by the Chinese National Standard - *GB-3095-2012 Ambient air quality standards* [59], the detail $PM_{2.5}$ pollution level classification described in Table 5.

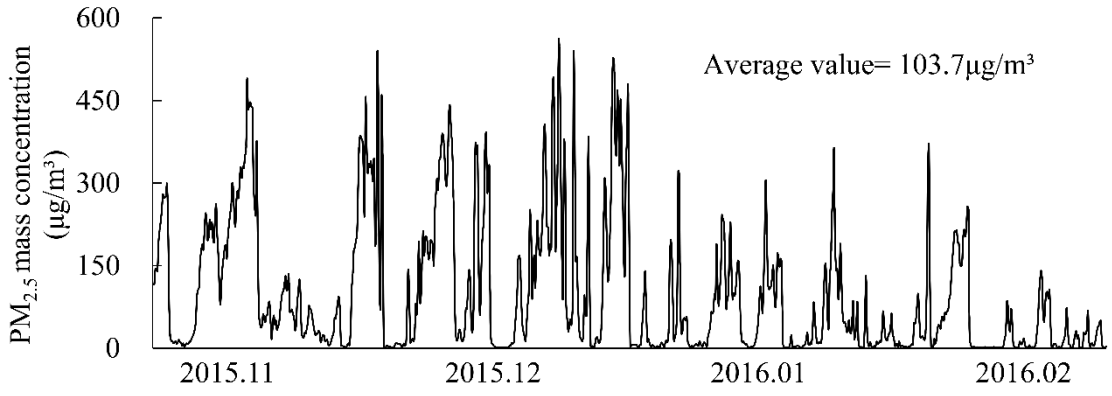

(a) Outdoor $PM_{2.5}$ hourly-average mass concentration in Beijing

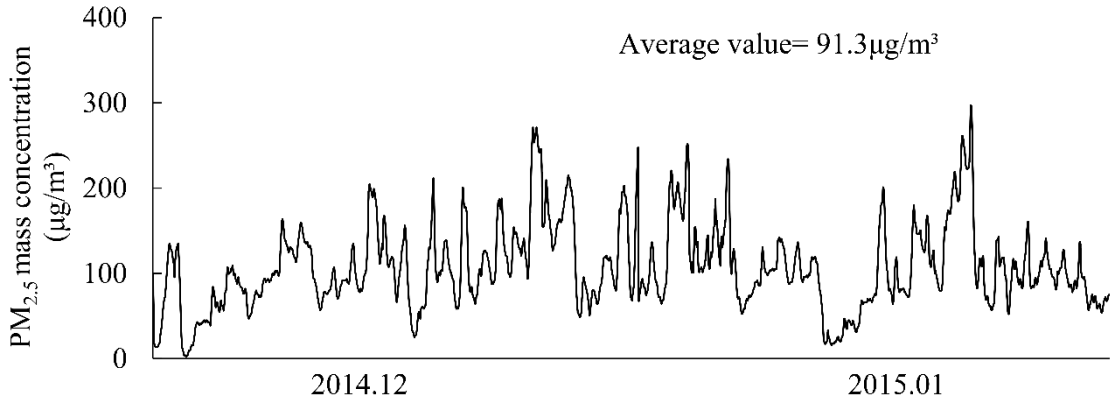

(b) Outdoor $PM_{2.5}$ hourly-average mass concentration in Guangzhou

Figure 5: Outdoor air quality during the monitoring period

Table 5: $PM_{2.5}$ pollution level classification in GB-3095-2012

Table 5

$PM_{2.5}$ pollution level	$PM_{2.5}$ mass concentration ($\mu g/m^3$)
Acceptable	0-75
Slightly polluted	75-115
Moderately polluted	115-150
Severely polluted	150-250
Seriously polluted	>250

3.1.4 Relationship between indoor and outdoor $PM_{2.5}$ mass concentrations

Figure 6a-6f compare both indoor and outdoor $PM_{2.5}$ mass concentrations for SP1-5 when the outdoor air quality was classified as acceptable, slightly/moderately polluted and severely/seriously polluted (since there was only one sampling site in Guangzhou, SP6 was not involved in comparison). Table 6 has listed some detailed data obtained from these figures. The results show that when outdoor air quality was classified as acceptable, the indoor air quality at all five sampling sites (mean C_{in}=25.8μg/m³, 20.5μg/m³, 27.7μg/m³, 22.2μg/m³, 21.8μg/m³, respectively) was also within the acceptable range (<75μg/m³) defined by the Chinese standard (shown in Figure 6a and 6b). Similarly, when the outdoor air quality was classified as slightly/moderately polluted, the indoor air quality at most sampling sites was also acceptable, except that at SP3 (mean C_{in}=70.9μg/m³, 56.9μg/m³, 79.7μg/m³, 69.6μg/m³, 65.8μg/m³, respectively, shown in Figure 6c and 6d). However, from here, a difference between sampling sites has started to appear. When the outdoor air quality was classified as severely/seriously polluted, the indoor air quality of all sampling sites exceeded the threshold (mean C_{in}=210.7μg/m³, 126.7μg/m³, 200.7μg/m³, 156.2μg/m³, 136.0μg/m³, respectively), and the exceeding levels are different between them (shown in Figure 6e and 6f).

The filed measurement results show a great difference of indoor air quality between the five sampling sites, under the same outdoor $PM_{2.5}$ pollution conditions. This phenomenon may be contributed by a combinational effect of both external window crack structure

and room dimension. In order to identify the individual influence of the two parameters, therefore, a method that can separate the two parameters is required.

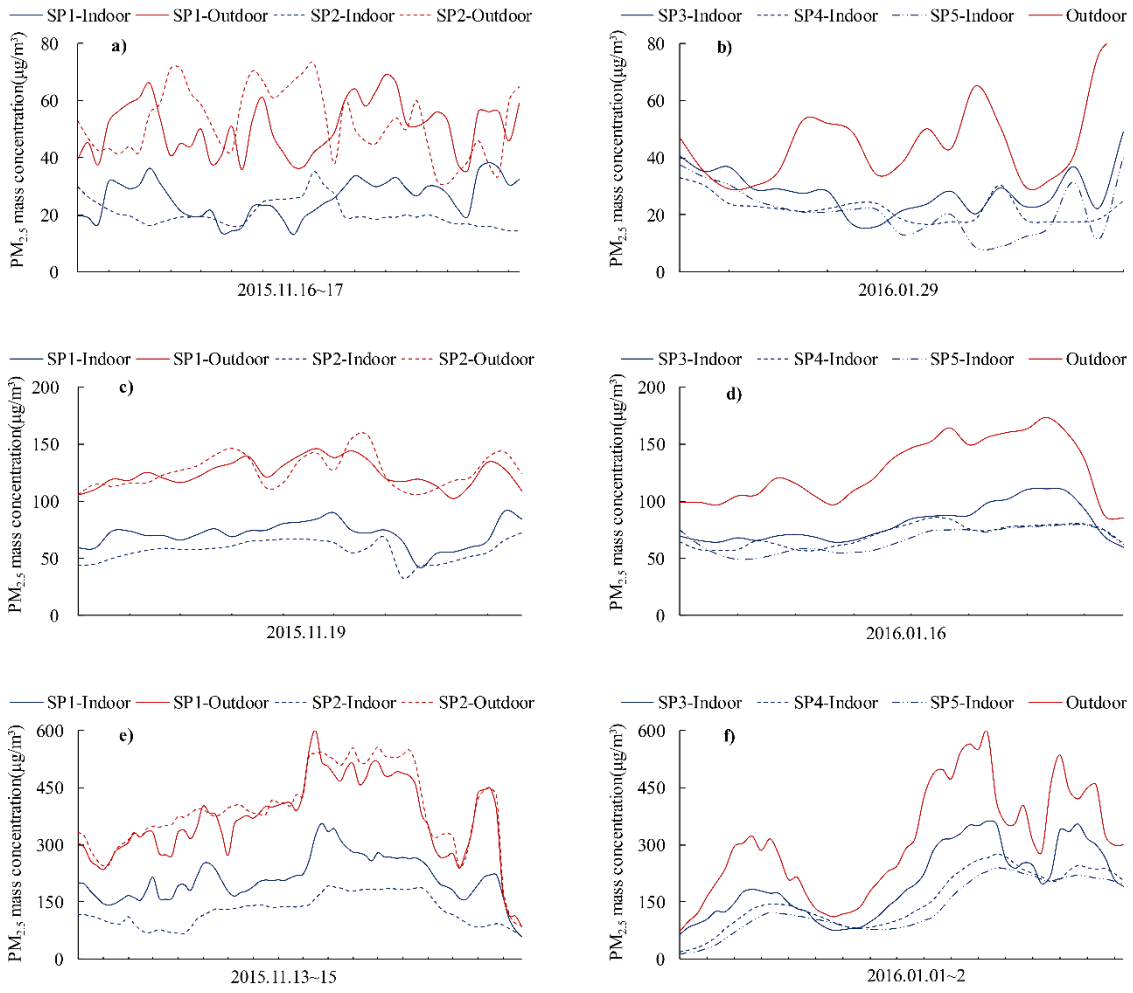

Figure 6: Indoor/outdoor $PM_{2.5}$ mass concentrations in different outdoor pollution level

Table 6: Mean Indoor/outdoor $PM_{2.5}$ mass concentrations in different outdoor pollution level from

Table 6

Sampling Site	Outdoor acceptable		Outdoor slightly/ moderately polluted		Outdoor severely/ seriously polluted	
	$\overline{C_{out}}$(μg/m³)	$\overline{C_{in}}$(μg/m³)	$\overline{C_{out}}$(μg/m³)	$\overline{C_{in}}$(μg/m³)	$\overline{C_{out}}$(μg/m³)	$\overline{C_{in}}$(μg/m³)
1	50.5	25.8	124.0	70.9	364.3	210.7
2	52.3	20.5	126.2	56.9	389.6	126.7
3	45.9	27.7	126.6	79.7	309.1	200.7
4	45.9	22.2	126.6	69.6	309.1	156.2
5	45.9	21.8	126.6	65.8	309.1	136.0

3.2 Model solution and validation

This study intended to use the related data (i.e. A_{Pi}, A_{ki} and A_i) from SP1-5 (located in Beijing) to solve the two unknowns (i.e. γ_1 and γ_2) in Equation 13, using the Least Square Solution method mentioned in Section 2.3. Then the model was validated against the data measured at SP6 (located in Guangzhou). Using the values listed in Table 1, the corresponding A_{Pi} and A_{ki} in Matrix 15 were calculated for all six sampling sites by Equation 9 and Equation 11. The values of A_i were estimated by statistical analysis of the field measurement data, using Equation 1, and the method has been detailed described by the authors in [18]. The calculation results for SP1-5 have been listed in Table 7, and these data were used in the study for solving the model. As described in Section 2.3, the Least Square Solution method was then be used to calculate γ_1 and γ_2 based on the calculated A_{Pi}, A_{ki} and A_i in Table 7, and then got γ_1=0.194 and γ_2=-0.221. The corresponding minimum residual sum of squares was calculated as $S(\boldsymbol{\gamma})_{min} = \|\boldsymbol{A\gamma} - \boldsymbol{b}\|^2 = 0.005$.

Table 7: Calculated values of A_P, A_k and A for the five sampling sites

Table 7

Sampling Site	A_P	A_k	A
1	0.018	0.443	0.576
2	0.009	0.547	0.422
3	0.017	0.371	0.603
4	0.013	0.315	0.520
5	0.012	0.664	0.474

Thus, Equation 13 becomes,

$$A = \left(\frac{d}{z}\right)^{0.194} \cdot \left(\frac{F_{wid}}{F_{fl}\left(\varphi_{ce} + \varphi_{fl}\right) + 2\left(F_{dep} + F_{wid}\right)\varphi_{ve}}\right)^{-0.221} \quad (18)$$

In order to validate the accuracy of the above equation, the data collected from SP6 were used. The values calculated by Equation 18 above and those calculated by the statistical analysis method mentioned in [18] have been compared in Table 8. The comparison shows a good agreement between the two values, with the relative error of 5.4%. Therefore, there is confidence that Equation 18 can give reliable results for real applications, even in different horizon, structure of external window crack and room dimension, as well as locations.

Table 8: Comparison of calculated coefficient *A* by two different methods

Table 8

Sampling Site	A_P	A_k	Calculated using Equation 18	Calculated using Equation1	Error
6	0.017	0.462	0.538	0.569	5.4%

Substituting Equation 18 into Equation 1 gives an updated version of the existing model mentioned in [18]. Apparently, the new version adopts more parameters related to the building (e.g. external window crack structure and room dimension) and this enhances the flexibility of the method developed already.

3.3 Model implementation

In order to demonstrate how the updated method can help real design applications, two scenarios have been proposed, as introduced in Section 3.3.1 and 3.3.2, respectively.

3.3.1 Sensitivity analysis of the effect of external window crack structure and room dimension on indoor $PM_{2.5}$ mass concentration

According to Section 3.1.4, various external window crack structures and room dimensions can affect the indoor air quality under the same outdoor conditions. In order to separately analyze the contribution of the two parameters, a sensitivity analysis has been employed, using the updated method in this study.

The sensitivity analysis was based on the controlling variable method, given as: when evaluating the influence of one parameter on the I/O ratio, its value was increased by 50% while keeping the other factors unchanged. Then the updated model was used to calculate the corresponding I/O ratio. Figure 7 shows the change of the I/O ratio when each parameter was changed. From the results, it could be found that the influence from the

external window crack structure (represented by d, z) was much stronger than that from the room dimension (represented by F_{dep}, F_{fl} and F_{wid}). The highest sensitive parameter was revealed to be the window crack height (d), with I/O ratio changing rates from 8.4%-10.3% for the six sampling sites. The second parameter was the window crack depth (z), with I/O ratio changing rates between 7.7% and 9.3%. The ranking for the remaining parameters was the depth area (F_{dep}), the floor area (F_{fl}), and then the width area (F_{wid}). From this result, it could be found that in order to provide better indoor air quality regarding to $PM_{2.5}$, more attentions should be paid on promoting the external window structure, rather than the room dimension.

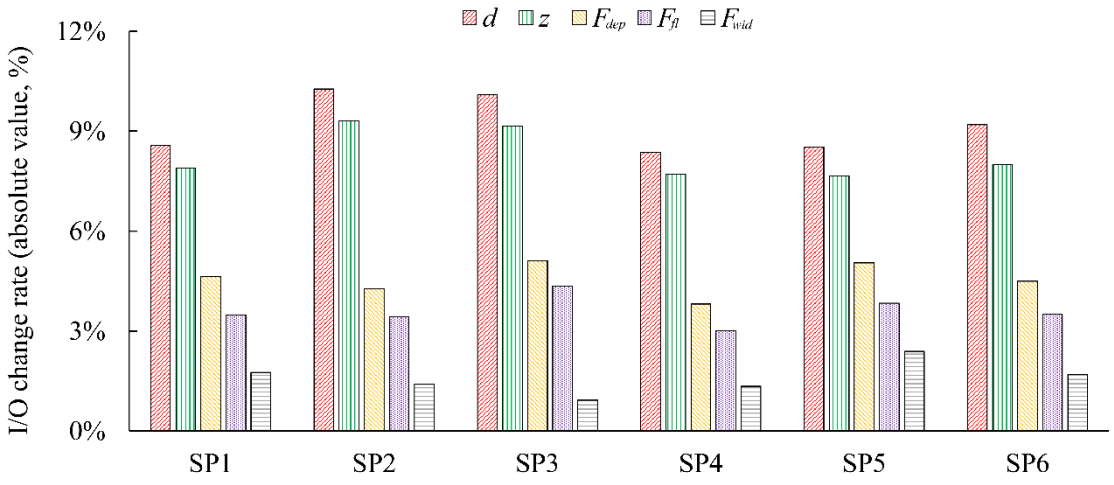

Figure 7: Sensitivity of I/O ratio to the parameters of external window crack structure and room dimension

3.3.2 Enhancing external window regarding to both crack structure and air-tightness level

In real building design applications, it may need to identify proper window air-tightness levels/window crack structure to achieve acceptable indoor air quality regarding to $PM_{2.5}$,

due to the high importance identified in the above section. In this section, SP1 was selected for the demonstration, and both its air-tightness level and window crack structure were changed, as shown in Table 9. The results reflect that with the increase of window air-tightness levels, the I/O ratio are decreased so an air-tighter window can help to promote the indoor air quality, which the impact can be quantified by the updated model from this study. Additionally, the I/O ratio also shows a downward trend with the decrease of the d/z when the windows are in the same air-tightness level, and this trend could be quantified using the updated model as well.

Table 9: Effect of various window air-tightness levels and crack structure on the I/O ratio

Table 9

Air-tightness level	z=50mm d (mm)	I/O decrease rate (%)	z=60mm d (mm)	I/O decrease rate (%)	z=70mm d (mm)	I/O decrease rate (%)
6	0.679-0.782 [a]	3.4-6.0	0.720-0.829	5.7-8.3	0.785-0.872	7.6-9.5
7	0.536-0.679	6.0-10.3	0.569-0.721	8.3-12.4	0.599-0.758	9.5-14.1
8	≤0.536	≥10.3	≤0.569	≥12.4	≤0.599	≥14.1

[a] All calculated ranges were obtained by the upper and lower bounds of q_l respectively, corresponding to its air-tightness level shown in Table 2.

4. Conclusion

In order to quantify the influence of the external window crack structure and some relevant parameters, such as room dimension and window air-tightness level, on the indoor $PM_{2.5}$ mass concentration, an existing model has been updated and introduced in this paper. The updated model includes parameters, including external window crack structure, room dimension and outdoor meteorological conditions, and can be used to

quantify the influence of changing external window crack structure, room dimension and window air-tightness level on the indoor $PM_{2.5}$ mass concentration. The model has been validated against the statistical analysis method to provide confidence on its accuracy. The model is based on the I/O ratio and should be able to help both theoretical analysis of building performance and also performance prediction, such as dynamic building performance simulation.

Acknowledgement:

This work was sponsored by the National Natural Science Foundation of China (No. 51378024), Beijing Municipal Natural Science Foundation (No. 8162006) and the 12th Five-Year Key Project, Ministry of Science and Technology of China (No. 2012BAJ02B02).

References:

[1] C.K. Chan, X. Yao, Air pollution in mega cities in China, Atmos Environ 42(1) (2008) 1-42.

[2] China Environmental Status Bulletin 2015. <http://www.mep.gov.cn/gkml/hbb/qt/201606/t20160602_353138.htm>, 2016 (accessed June 2.2016).

[3] W.H. Organization, Air quality guidelines - global update 2005, Public Health & Environment (2014).

[4] Z.H. Chen, Y.F. Wu, P.L. Wang, Y.P. Wu, Z.Y. Li, Y. Zhao, J.S. Zhou, C. Zhu, C. Cao, Y.Y. Mao, F. Xu, B.B. Wang, S.A. Cormier, S.M. Ying, W. Li, H.H. Shen, Autophagy is essential for ultrafine particle-induced inflammation and mucus hyperproduction in airway epithelium, Autophagy 12(2) (2016) 297-311.

[5] C. Chen, B. Zhao, Review of relationship between indoor and outdoor particles: I/O ratio, infiltration factor and penetration factor, Atmos Environ 45(2) (2011) 275-288.

[6] S. Pan, C. Xu, S. Wei, T.M. Hassan, L. Xie, Y. Xiong, S. Firth, D. Greenwood, P.D. Wilde, Improper window use in office buildings: findings from a longitudinal study in Beijing, China, Energy Procedia 88 (2016) 761-767.

[7] O. Hanninen, G. Hoek, S. Mallone, E. Chellini, K. Katsouyanni, C. Gariazzo, G. Cattani, A. Marconi, P. Molnar, T. Bellander, M. Jantunen, Seasonal patterns of outdoor PM infiltration into indoor environments: review and meta-analysis of available studies from different climatological zones in Europe, Air Qual Atmos Hlth 4(3-4) (2011) 221-233.

[8] Y.C. Hong, X.C. Pan, S.Y. Kim, K. Park, E.J. Park, X.B. Jin, S.M. Yi, Y.H. Kim, C.H. Park, S. Song, H.

Kim, Asian Dust Storm and pulmonary function of school children in Seoul, Science of the Total Environment 408(4) (2010) 754-759.
[9] Q. Zhang, Y. Zhu, Characterizing ultrafine particles and other air pollutants at five schools in South Texas, Indoor Air 22(1) (2012) 33-42.
[10] A. Zwozdziak, I. Sowka, B. Krupinska, J. Zwozdziak, A. Nych, Infiltration or indoor sources as determinants of the elemental composition of particulate matter inside a school in Wroclaw, Poland?, Build Environ 66 (2013) 173-180.
[11] I. Rivas, M. Viana, T. Moreno, L. Bouso, M. Pandolfi, M. Alvarez-Pedrerol, J. Forns, A. Alastuey, J. Sunyer, X. Querol, Outdoor infiltration and indoor contribution of UFP and BC, OC, secondary inorganic ions and metals in PM2.5 in schools, Atmos Environ 106 (2015) 129-138.
[12] M. Elbayoumi, N.A. Ramli, N.F.F.M. Yusof, Spatial and temporal variations in particulate matter concentrations in twelve schools environment in urban and overpopulated camps landscape, Build Environ 90 (2015) 157-167.
[13] E. Diapouli, A. Chaloulakou, N. Mihalopoulos, N. Spyrellis, Indoor and outdoor PM mass and number concentrations at schools in the Athens area, Environ Monit Assess 136(1-3) (2008) 13-20.
[14] M. Branis, P. Rezacova, M. Domasova, The effect of outdoor air and indoor human activity on mass concentrations of PM10, PM2.5, and PM1 in a classroom, Environmental Research 99(2) (2005) 143-149.
[15] V.S. Chithra, S.M.S. Nagendra, Indoor air quality investigations in a naturally ventilated school building located close to an urban roadway in Chennai, India, Build Environ 54 (2012) 159-167.
[16] S.E. Chatoutsidou, J. Ondracek, O. Tesar, K. Torseth, V. Zdimal, M. Lazaridis, Indoor/outdoor particulate matter number and mass concentration in modern offices, Build Environ 92 (2015) 462-474.
[17] H.W. Kuo, H.Y. Shen, Indoor and outdoor PM2.5 and PM10 concentrations in the air during a dust storm, Build Environ 45(3) (2010) 610-614.
[18] L. Zhao, C. Chen, P. Wang, Z.G. Chen, S.J. Cao, Q.Q. Wang, G.Y. Xie, Y.L. Wan, Y.F. Wang, B. Lu, Influence of atmospheric fine particulate matter (PM2.5) pollution on indoor environment during winter in Beijing, Build Environ 87 (2015) 283-291.
[19] Y.H. Zhu, L.X. Yang, C.P. Meng, Q. Yuan, C. Yan, C. Dong, X. Sui, L. Yao, F. Yang, Y.L. Lu, W.X. Wang, Indoor/outdoor relationships and diurnal/nocturnal variations in water-soluble ion and PAH concentrations in the atmospheric PM2.5 of a business office area in Jinan, a heavily polluted city in China, Atmos Res 153 (2015) 276-285.
[20] Y. Li, L. Chen, D.M. Ngoc, Y.P. Duan, Z.B. Lu, Z.H. Wen, X.Z. Meng, Polybrominated Diphenyl Ethers (PBDEs) in PM2.5, PM10, TSP and Gas Phase in Office Environment in Shanghai, China: Occurrence and Human Exposure, Plos One 10(3) (2015).
[21] P.S. Hung, H.Y. Shen, H.W. Kuo, Factors affecting the indoor concentrations of PM2.5 and PM10 in a high-rise office building, Epidemiology 17(6) (2006) S355-S356.
[22] M.S. Zuraimi, Z.C. Tan, Impact of residential building regulations on reducing indoor exposures to outdoor PM2.5 in Toronto, Build Environ 89 (2015) 336-344.
[23] H. Krasnov, I. Katra, V. Novack, A. Vodonos, M.D. Friger, Increased indoor PM concentrations controlled by atmospheric dust events and urban factors, Build Environ 87 (2015) 169-176.
[24] D. Massey, J. Masih, A. Kulshrestha, M. Habil, A. Teneja, Indoor/outdoor relationship of fine particles less than 2.5 mu m (PM2.5) in residential homes locations in central Indian region, Build Environ 44(10) (2009) 2037-2045.
[25] D. Massey, A. Kulshrestha, J. Masih, A. Taneja, Seasonal trends of PM10, PM5.0, PM2.5 & PM1.0 in indoor and outdoor environments of residential homes located in North-Central India, Build Environ 47 (2012) 223-231.

[26] M.S. Breen, T.C. Long, B.D. Schultz, R.W. Williams, J. Richmond-Bryant, M. Breen, J.E. Langstaff, R.B. Devlin, A. Schneider, J.M. Burke, S.A. Batterman, Q.Y. Meng, Air Pollution Exposure Model for Individuals (EMI) in Health Studies: Evaluation for Ambient PM2.5 in Central North Carolina, Environmental Science & Technology 49(24) (2015) 14184-14194.
[27] C.H. Tseng, H.C. Wang, N.Y. Xiao, Y.M. Chang, Examining the feasibility of prediction models by monitoring data and management data for bioaerosols inside office buildings, Build Environ 46(12) (2011) 2578-2589.
[28] P. Goyal, A.T. Chan, N. Jaiswal, Statistical models for the prediction of respirable suspended particulate matter in urban cities, Atmos Environ 40(11) (2006) 2068-2077.
[29] Y. Han, M. Qi, Y.L. Chen, H.Z. Shen, J. Liu, Y. Huang, H. Chen, W.X. Liu, X.L. Wang, J.F. Liu, B.S. Xing, S. Tao, Influences of ambient air PM2.5 concentration and meteorological condition on the indoor PM2.5 concentrations in a residential apartment in Beijing using a new approach, Environmental Pollution 205 (2015) 307-314.
[30] T. Schneider, K.A. Jensen, P.A. Clausen, A. Afshari, L. Gunnarsen, P. Wahlin, M. Glasius, F. Palmgren, O.J. Nielsen, C.L. Fogh, Prediction of indoor concentration of 0.5-4 mu m particles of outdoor origin in an uninhabited apartment, Atmos Environ 38(37) (2004) 6349-6359.
[31] V.S. Chithra, S.M.S. Nagendra, Characterizing and predicting coarse and fine particulates in classrooms located close to an urban roadway, Journal of the Air & Waste Management Association 64(8) (2014) 945-956.
[32] D.L. Liu, W.W. Nazaroff, Modeling pollutant penetration across building envelopes, Atmos Environ 35(26) (2001) 4451-4462.
[33] L.W. Tian, G.Q. Zhang, Y.L. Lin, J.H. Yu, J. Zhou, Q. Zhang, Mathematical model of particle penetration through smooth/rough building envelop leakages, Build Environ 44(6) (2009) 1144-1149.
[34] C. Chen, B. Zhao, W.T. Zhou, X.Y. Jiang, Z.C. Tan, A methodology for predicting particle penetration factor through cracks of windows and doors for actual engineering application, Build Environ 47 (2012) 339-348.
[35] W.J. Ji, B. Zhao, Contribution of outdoor-originating particles, indoor-emitted particles and indoor secondary organic aerosol (SOA) to residential indoor PM2.5 concentration: A model-based estimation, Build Environ 90 (2015) 196-205.
[36] J.M. Burke, M.J. Zufall, H. Ozkaynak, A population exposure model for particulate matter: case study results for PM2.5 in Philadelphia, PA, J Expo Anal Env Epid 11(6) (2001) 470-489.
[37] C. Chen, Z. Chen, P. Wang, S. Wei, H. Qin, Y. Wan, Y. Wang, Impact of different airtightness of external windows on indoor air quality with respect to PM2.5 pollution, The 7th International Conference on Sustainable Development in Building and Environment, Reading, UK., 2015.
[38] E. Diapouli, A. Chaloulakou, P. Koutrakis, Estimating the concentration of indoor particles of outdoor origin: A review, Journal of the Air & Waste Management Association 63(10) (2013) 1113-1129.
[39] Y.G. Li, Z.D. Chen, A balance-point method for assessing the effect of natural ventilation on indoor particle concentrations, Atmos Environ 37(30) (2003) 4277-4285.
[40] G. Levermore, T. Muneer, C. Sanders, J. Page, CIBSE Guide A Environmental design, Academic Press (2006).
[41] M.I. Montoya, E. Pastor, E. Planas, Air infiltration in Catalan dwellings and sealed rooms: An experimental study, Fuel & Energy Abstracts 46(10) (2011) 2003-2011.
[42] S. Shi, C. Chen, B. Zhao, Air Infiltration Rate Distributions of Residences in Beijing, Building and Environment 92 (2015) 528–537.
[43] C. Younes, C.A. Shdid, G. Bitsuamlak, Air infiltration through building envelopes: A review, Journal

of Building Physics 35(3) (2012) 267-302.
[44] H.B. Awbi, Ventilation of Buildings (Second Edition), Taylor & Francis Group, USA, 2003.
[45] D.L. Liu, W.W. Nazaroff, Particle penetration through building cracks, Aerosol Sci Tech 37(7) (2003) 565-573.
[46] C.J. Jeng, W.B. Kindzierski, D.W. Smith, Particle penetration through rectangular-shaped cracks, J Environ Eng Sci 5 (2006) S111-S119.
[47] C.J. Jeng, W.B. Kindzierski, D.W. Smith, Particle penetration through inclined and L-shaped cracks, J Environ Eng-Asce 133(3) (2007) 331-339.
[48] T.L. Thatcher, M.M. Lunden, K.L. Revzan, R.G. Sextro, N.J. Brown, A concentration rebound method for measuring particle penetration and deposition in the indoor environment, Aerosol Sci Tech 37(11) (2003) 847-864.
[49] T.L. Thatcher, A.C.K. Lai, R. Moreno-Jackson, R.G. Sextro, W.W. Nazaroff, Effects of room furnishings and air speed on particle deposition rates indoors, Atmos Environ 36(36) (2002) 1811-1819.
[50] H. Lu, L. Lu, A numerical study of particle deposition in ribbed duct flow with different rib shapes, Build Environ 94 (2015) 43-53.
[51] P.H. Baker, S. Sharples, I.C. Ward, Air-Flow through Cracks, Build Environ 22(4) (1987) 293-304.
[52] L. Popescu, K. Limam, Particle penetration research through buildings' cracks, Hvac&R Res 18(3) (2012) 312-322.
[53] C.R. He, L. Morawska, D. Gilbert, Particle deposition rates in residential houses, Atmos Environ 39(21) (2005) 3891-3899.
[54] R.Y. You, B. Zhao, C. Chen, Developing an Empirical Equation for Modeling Particle Deposition Velocity onto Inclined Surfaces in Indoor Environments, Aerosol Sci Tech 46(10) (2012) 1090-1099.
[55] M. Abadie, K. Limam, F. Allard, Indoor particle pollution: effect of wall textures on particle deposition, Build Environ 36(7) (2001) 821-827.
[56] R.A. Horn, C.R. Johnson, Matrix analysis, 2 ed., Cambridge University Press, USA, 2013.
[57] GB/T 7106-2008 Graduations and test methods of air permeability, watertightness, wind load resistance performance for building external windows and doors, Standardization Administration of the People's Republic of China, 2008.
[58] R.A.C. Engineers, 1997 ASHRAE handbook : fundamentals, ASHRAE1997.
[59] GB 3095-2012 Ambient air quality standards, Ministry of Environment Protection of the People's Republic of China; General Administration of Quality Supervision, Inspection and Quarantine of the People's Republic of China, 2012.